Proceedings of the 11th World Congress on Electrical Engineering and Computer Systems and Sciences (EECSS'25)
Paris, France - August, 2025
Paper No. ICBES 146
DOI: 10.11159/icbes25.146

Mirror: Embedded AI Mirror for Thermal Tumor Screening and Remote Monitoring

Wissal EL HABTI[1], Abdellah AZMANI[2], Jabir EL AARAJ[3], Mohcine BENNANI MECHITA4
[1]Intelligent Automation & BiomedGenomics Laboratory, Faculty of Science and Technology of Tangier, Abdelmalek Essaadi University.
Tangier, Morocco.
wissal.elhabti@etu.uae.ac.ma ; a.azmani@uae.ac.ma
[2] Intelligent Automation & BiomedGenomics Laboratory, Faculty of Science and Technology of Tangier, Abdelmalek Essaadi University.
Tangier, Morocco.
mbennani@uae.ac.ma

Abstract **-** This paper presents *mIRror*, a modular intelligent mirror system designed to support autonomous tumor screening through thermal imaging in both clinical and remote settings. The system integrates embedded long-wave infrared (LWIR) sensing, real-time thermal preprocessing, lightweight convolutional neural inference, and onboard result visualization within a compact edge device. Its design addresses key challenges in accessibility, repeatability, and privacy, offering an alternative to conventional imaging methods in low-resource or decentralized environments.
The clinical workflow is structured around standardized thermal acquisition protocols that ensure consistent patient positioning, controlled environmental conditions, and reproducible image capture. The processing chain encompasses thermal calibration, region-of-interest segmentation, and real-time classification executed locally on embedded hardware. This configuration enables low-latency inference without reliance on external servers, preserving data confidentiality and supporting future scalability. To validate the system's diagnostic module, six lightweight convolutional models—including MobileNetV2, MobileNetV3 (Small and Large), EfficientNetB0, EfficientNetV2B0, and NASNetMobile—were trained and evaluated using the publicly available DMR-IR dataset. Models were assessed using AUC-ROC, precision-recall metrics, and statistical significance testing via the Friedman test and Nemenyi post-hoc analysis. MobileNetV3-Large demonstrated superior performance (AUC = 0.99) with consistent interpretability through Smooth Grad-CAM++ visualizations. While hardware prototyping is ongoing, these results provide a proof-of-concept for mIRror's embedded diagnostic capabilities. The modular architecture is designed to support future extensions, including federated learning for secure collaborative training and digital twin integration for individualized monitoring. Together, these components position *mIRror* as a scalable platform for AI-assisted thermal diagnostics.

Keywords**:** *Infrared Thermography, Edge Computing, Lightweight Convolutional Networks, Embedded Diagnostic Systems, Breast Cancer Screening, Federated Learning, Digital Twin.*

1. Introduction

Cancer screening is a critical pillar of global health strategies, significantly improving survival outcomes when diseases are caught in the early stages[1]. Conventional diagnostic tools such as mammography, colonoscopy, and low-dose CT have become essential to clinical workflows and early intervention[2]. Despite the widespread adoption of screening technologies, persistent disparities remain regarding their accessibility, diagnostic performance, and cultural acceptability across patient populations[3]. In recent years, there has been a growing emphasis on patient-centered screening paradigms, which advocate for individualized risk assessments, tailored communication, and shared clinical decision-making. As emphasized by [4], advancing this approach necessitates not only technical tools to support preference-sensitive care but also a broader cultural reorientation—one that recognizes that cancer screening decisions may not always yield a universally optimal solution.

Nonetheless, conventional diagnostic tools have well-recognized limitations. Mammography, although considered the standard approach for breast cancer screening, does not perform equally across all patient groups. While its sensitivity is high in fatty breast tissue, it drops substantially in extremely dense breasts—ranging between 30% and 48% in reported studies [5], [6], [7]. Additionally, as many as one in four breast cancers detected through screening may never progress, leading to overdiagnosis and overtreatment[8]. These diagnostic shortcomings can limit the effectiveness of screening in certain populations and reinforce broader disparities in health outcomes. Infrastructural constraints, exposure to ionizing radiation, and discomfort during procedures also pose barriers to widespread, repeatable, or decentralized use—especially in low-resource and remote settings. Some studies have suggested that digital infrared thermal imaging (DITI) may provide additional diagnostic information in dense breast tissue or among younger women, warranting further investigation[9].

Infrared (IR) thermography, a non-invasive modality capable of detecting surface-level temperature anomalies linked to physiological changes, is one such candidate[10]. IR systems offer real-time insights without radiation exposure by mapping thermal patterns caused by inflammation, vascular remodeling, or tumor metabolism. When coupled with artificial intelligence (AI), their diagnostic capacity is significantly enhanced. Deep learning models have achieved accuracies between 85% and 94% when classifying benign and malignant lesions—particularly effective in dense tissue where mammography underperforms[11], [12].

To build on these advances, we present a modular intelligent mirror system that integrates IR imaging, AI inference, federated learning, and digital twin modeling. This platform is designed for both in-clinic and remote deployment, offering real-time diagnostics while preserving patient privacy and adaptability. Although breast cancer is used as a representative use case, the architecture supports broader screening applications across multiple cancer types and thermally observable conditions.

2. mIRror Clinical workflow overview

The intelligent mirror system has been developed with a modular design that reflects the sequential steps of its clinical use—from capturing thermal images to generating interpretative results. Its architecture is intended to function reliably across different settings, including conventional clinics and remote care environments. Embedded processing capabilities allow for real-time analysis directly within the device without relying on external computation. As illustrated in Figure 1, the system is organized into distinct yet integrated components that align with key stages of the screening workflow: image acquisition, thermal preprocessing, AI-assisted inference, and result communication. Each component is designed to operate in coordination with the others, supporting consistency and adaptability across use cases. The following sections describe each phase of the workflow and its role in supporting clinical decision-making.

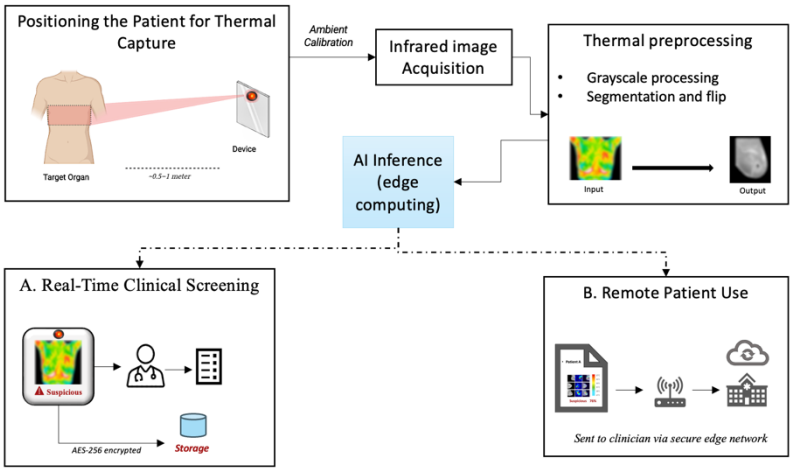

Fig. 1: mIRror Clinical Workflow.

2.1. Positioning the Patient for Thermal Capture

Accurate thermal imaging begins with precise and standardized patient positioning, a critical factor for minimizing artifacts and enhancing diagnostic consistency. In thermal imaging systems, particularly those integrated into embedded diagnostic devices, the quality of captured thermograms is susceptible to both physiological variability and environmental perturbations. To ensure reproducibility, the clinical setting is carefully controlled: ambient temperature is maintained between 22°C and 24°C with relative humidity below 50%, stabilizing cutaneous thermoregulation and reducing the influence of vasomotor fluctuations[13]. Before imaging, patients are advised to remove clothing and any accessories from the region of interest to avoid interference with heat distribution. A brief rest period of 10 to 15 minutes in a controlled environment is recommended to allow the skin surface temperature to stabilize. This acclimatization ensures that superficial blood flow reaches a steady state, reducing physiological variability and enhancing the accuracy of thermal measurements[14], [15].

In the breast screening use case, the patient is approximately 1.0 m from the infrared mirror, adopting a posture with arms elevated at a 90° angle from the torso[16]. This configuration minimizes occlusion from skin folds and exposes key anatomical landmarks, including the axillary regions, which are relevant for lymphatic assessment. The system integrates visual alignment tools to ensure consistency in pose across sessions. In clinical settings, alignment is confirmed manually by trained staff. In remote deployments, we aim to incorporate augmented reality (AR) overlays onto the mirror interface to assist patients in achieving proper positioning at home, thereby approximating the guidance typically provided in clinical settings.

In addition to spatial alignment, pre-imaging preparation protocols are essential for preserving the integrity of thermographic data. Patients are instructed to avoid physical exertion, caffeine, nicotine, and hot beverages for at least two hours before imaging. Skin should be free of lotions, powders, deodorants, or cosmetics, as these may interfere with infrared signal quality. Residuals may be removed using alcohol-free wipes, while thermal gels or enhancers are contraindicated under current clinical protocols[17].

2.2. Infrared Image Acquisition

The infrared (IR) imaging module in the intelligent mirror system captures thermal radiation passively emitted by the human body. Human skin, with an emissivity close to 0.98, behaves similarly to a blackbody in the thermal infrared range, allowing for precise measurement of surface temperature distributions[18]. The system operates in the long-wave infrared (LWIR) band, typically between 8 and 14 μm, where thermal emission is most significant under physiological conditions. Thermal emission at a given wavelength and temperature is governed by Planck's radiation law as shown in Eq. (1), where $L(\lambda,T)$ is spectral radiance, h is Planck's constant, c is the speed of light, k is Boltzmann's constant, λ is the wavelength, and T is the absolute temperature[19].

The system integrates an uncooled microbolometer sensor, which operates by detecting thermal radiation-induced resistance changes—a principle well-established in early infrared imaging research. Recent works have further optimized these sensors through improved NETD (<50 mK) and enhanced calibration algorithms, reinforcing their suitability for embedded diagnostic applications [20], [21].

2.3. Thermal preprocessing

Pre-processing transforms raw thermal images into standardized inputs for AI inference by correcting variability due to environmental noise, patient posture, and sensor drift. First, thermal data is linearly normalized into an 8-bit grayscale image as shown in Eq. (2).

$$L(\lambda,T)=\frac{2hc^2}{\lambda^5}\cdot\frac{1}{e^{\frac{hc}{\lambda kT}-1}} \tag{1}$$

$$I = 255 \cdot \frac{T - T_{min}}{T_{max} - T_{min}} \quad (2)$$

with T_{min} and T_{max} typically set between 30–40°C. This enhances contrast and facilitates consistent model input.

Orientation correction is then applied using landmark-based alignment to reduce postural variance. Region-of-interest (ROI) segmentation follows, isolating the anatomical target and masking background elements to reduce noise [22].Minimal on-device augmentation (e.g., slight shifts or brightness scaling) improves robustness during model training while preserving real-time execution.

2.4. AI edge inference and use case

The intelligent mirror system under development is intended to support two primary clinical pathways: **(A)** real-time screening in clinical settings and **(B)** remote patient monitoring. In both cases, thermal image classification is executed directly on the device via embedded edge computing. Local inference reduces latency and eliminates reliance on external servers, improving data security and responsiveness—critical features in decentralized healthcare environments [23].

In the clinical workflow (Use Case A), diagnostic outputs are generated on-site and reviewed immediately by the attending physician. For remote deployment (Use Case B), encrypted inference outputs or feature embeddings are transmitted to clinical endpoints for asynchronous review. To support efficient edge deployment, a lightweight convolutional neural network will be integrated into the system.

Looking ahead, two components are planned to enhance the system's adaptability and personalization. A federated learning framework will be implemented to enable secure, decentralized model updates across multiple devices without transmitting raw data [24]. Additionally, a digital twin module will be incorporated to simulate individual patient thermal and physiological dynamics, facilitating longitudinal tracking and personalized diagnostics [25]. Collectively, these enhancements position the intelligent mirror as a modular and secure diagnostic platform, capable of supporting both in-clinic workflows and remote patient monitoring across diverse healthcare environments.

3. Embedded System Design and Processing Chain

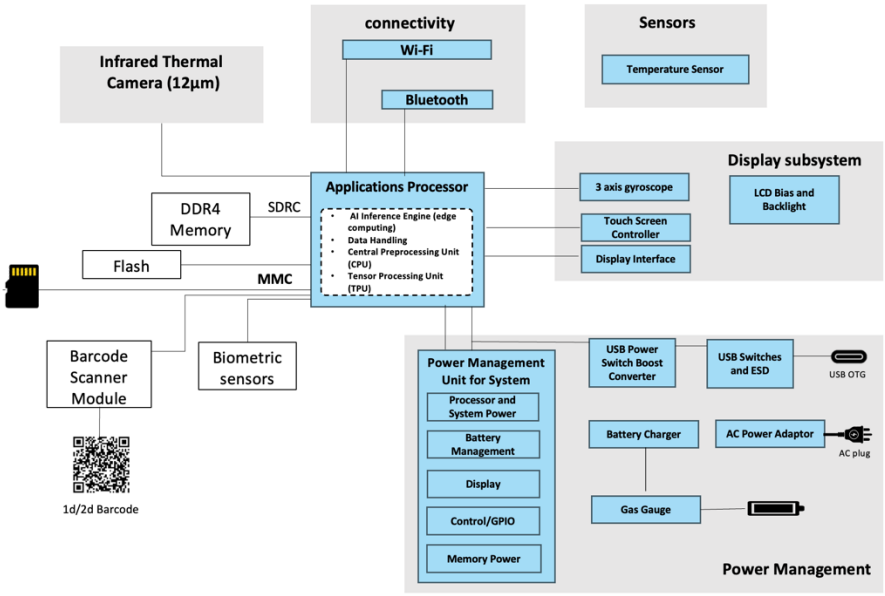

Fig. 2: System architecture diagram of the embedded hardware and processing chain within the infrared mirror.

The intelligent mirror platform integrates thermal sensing, signal processing, connectivity, and user interface modules into a compact embedded system designed for point-of-care screening. As depicted in Figure 2, the architecture is composed of four principal subsystems: (1) thermal acquisition, (2) embedded computation, (3) wireless communication, and (4) display and user interaction. The sensing module is based on an uncooled long-wave infrared (LWIR) microbolometer operating within the 8–14 μm spectral range, offering high thermal sensitivity and passive operation suitable for clinical environments.

Thermal image streams are routed to a central processing unit that includes specialized components for low-latency data handling and frame analysis. The system incorporates both volatile (DDR4) and non-volatile (eMMC and Flash) memory units for efficient data buffering and retention. Barcode scanning and biometric recognition modules are integrated for patient identification and workflow streamlining.

Wireless transmission capabilities via Wi-Fi and Bluetooth enable synchronized data exchange with external health records systems or telemedicine platforms. Diagnostic results and real-time thermal maps are visualized through an embedded touchscreen display governed by a dedicated display controller. Power delivery is managed by a multi-tiered unit responsible for regulating processor activity, display output, and battery health. The modular design of the system facilitates future augmentation with distributed learning frameworks and patient-specific simulation tools, supporting adaptive monitoring across temporal scales.

4. AI Model Evaluation for Embedded Thermal Inference

This section outlines the experimental protocol and findings from the performance assessment of compact convolutional neural architectures applied to thermal image classification using the DMR-IR dataset. The experiments emulate the operational context envisioned for the mIRror system, offering a preliminary validation of the embedded inference framework currently in development.

4.1. Dataset

All experiments were conducted on the DMR-IR dataset [26], an open-access thermal breast imaging repository developed to support the assessment of artificial intelligence techniques in diagnostic contexts. The dataset includes infrared thermograms, digitized mammograms, and associated clinical metadata collected from 141 patients at the Hospital Universitário Antônio Pedro (HUAP), part of the Fluminense Federal University in Brazil. In total, it contains 3,534 infrared images.

Each thermogram was acquired under controlled clinical conditions and annotated as either malignant, benign, or normal, providing a structured ground truth for supervised learning. The dataset was selected based on its class diversity, relevance to real-world screening scenarios, and established use in prior studies involving thermal image analysis.

4.2. Preprocessing and Augmentation

Preprocessing followed the thermal normalization and alignment protocol described previously in Section 3. During training, additional data augmentation was applied to improve model generalization and reduce overfitting. Augmentations included random horizontal flipping, contrast variation, and slight rotations. All input images were resized to 224×224 pixels and processed in batches using TensorFlow's real-time augmentation pipeline.

4.3. Model Selection and Training Configuration

Given the resource constraints of embedded hardware, we selected six lightweight CNN architectures for comparison: MobileNetV2 [27], MobileNetV3-Small [28], MobileNetV3-Large [28], EfficientNetB0 [29], EfficientNetV2B0 [30], and NASNetMobile [31]. All models were initialized with pretrained ImageNet weights and fine-tuned on the DMR-IR dataset using the Adam optimizer (learning rate = 1e-4), batch size of 16, and trained for 50 epochs with categorical cross-entropy loss. The experimental pipeline was designed to emulate edge deployment environments and ensure a consistent training setup across all models.

4.4. Results and Interpretability

The comparative assessment of six lightweight convolutional architectures underscored marked disparities in computational efficiency and classification behavior. MobileNetV3Small achieved the lowest inference latency (1.18 s), closely followed by MobileNetV2 (1.30 s) and MobileNetV3Large (1.41 s). By contrast, NASNetMobile, despite its compact design, exhibited the longest processing time (4.19 s), suggesting suboptimal computational scalability.

A **Friedman test** confirmed statistically significant performance variations among the models ($\chi^2 = 195.626$, $p < 0.0001$), and the subsequent **Nemenyi post-hoc test** identified EfficientNetV2B0 as significantly superior to its counterparts ($p < 0.05$), while MobileNetV3Small and NASNetMobile consistently ranked among the lowest-performing configurations.

These outcomes were consistent with the grouped evaluation metrics reported in Figure 3a, where EfficientNetV2B0 delivered consistently high scores across accuracy, precision, recall, F1-score, and ROC AUC, indicating balanced predictive behavior. Conversely, MobileNetV3Small exhibited a degenerate classification pattern—nearly always predicting the malignant class—which resulted in a recall-biased profile and reduced discriminative value. NASNetMobile similarly suffered from one-sided predictions, yielding diminished overall performance and low reliability despite a prolonged training schedule. Notably, both models displayed stagnation in validation accuracy during training, further evidencing convergence deficiencies under identical optimization settings. In contrast, EfficientNetV2B0 not only sustained optimal training stability but also demonstrated strong generalization, positioning it as the most suitable candidate for deployment in clinical screening environments.

To elucidate the decision-making behavior of the top-performing models, **Smooth Grad-CAM++** was applied to representative benign and malignant samples (Figure 3b–d). EfficientNetV2B0 (Figure 3b) generated moderately informative attribution maps, with salient regions partially covering thermally irregular areas, though exhibiting some spatial dispersion. MobileNetV3Large (Figure 3c) produced the most diagnostically aligned activations, consistently localizing high-intensity regions corresponding to plausible tumor sites, thus demonstrating superior spatial sensitivity and clinical relevance. In contrast, MobileNetV2 (Figure 3d) yielded diffuse and less focused saliency maps, reflecting broader activation patterns with reduced anatomical specificity. These results suggest that MobileNetV3Large offers not only competitive predictive performance but also enhanced interpretability, reinforcing its suitability for deployment in thermography-based breast cancer screening workflows.

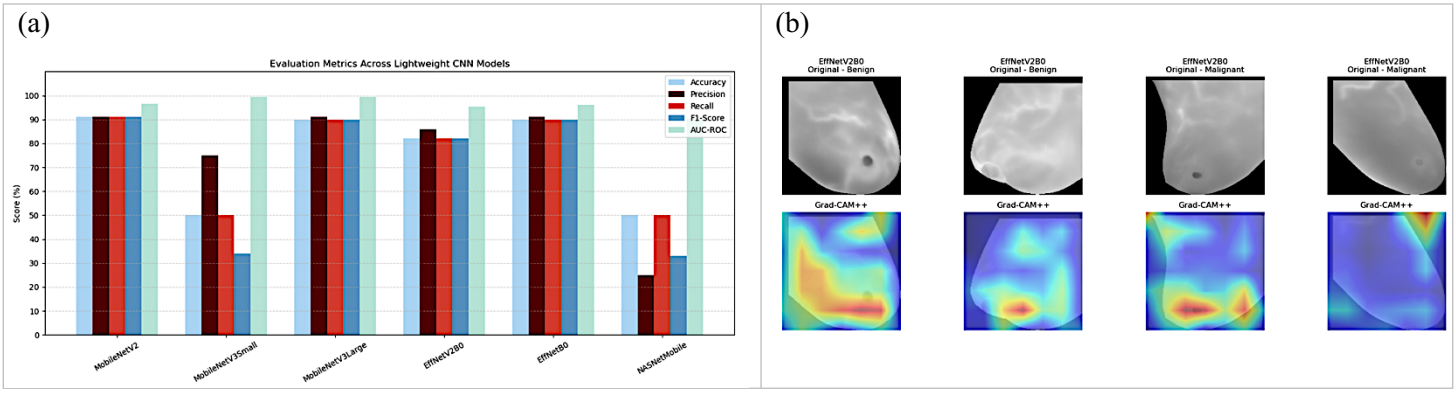

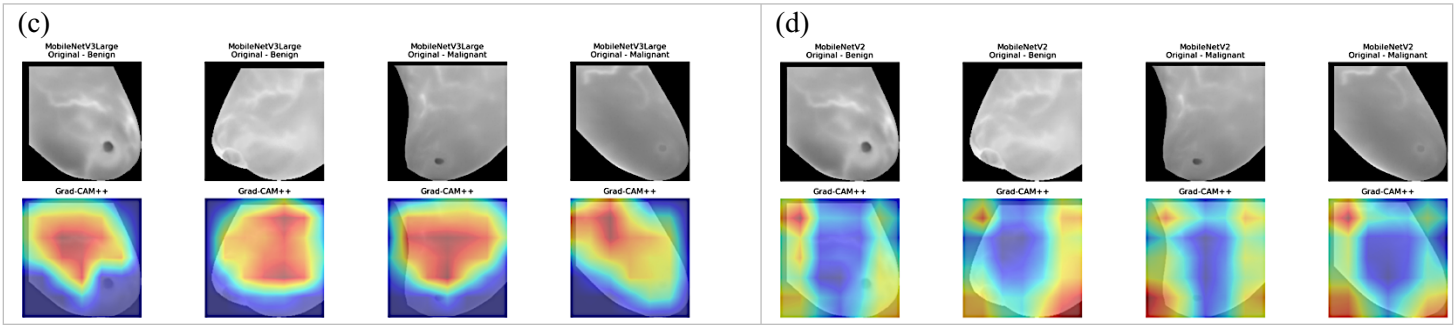

Fig. 3. Evaluation metrics (a) and Smooth Grad-CAM++ visual explanations (b–d) for EfficientNetV2B0, MobileNetV3Large, and MobileNetV2, highlighting predictive performance and thermographic localization.

4. Conclusion

This work introduced *mIRror*, a thermographic mirror system designed to perform autonomous tumor screening and monitoring at the edge. Through an experimental assessment of six lightweight convolutional models, MobileNetV3Large emerged as the most dependable architecture, offering a strong balance between classification performance, inference efficiency, and interpretability. These findings highlight the importance of selecting architectures suited to thermal image modalities, especially under hardware constraints. Looking ahead, efforts will concentrate on tailoring a dedicated lightweight model that can be adapted across different cancer types. Additionally, the system will incorporate federated learning to support secure multi-institutional collaboration and adopt digital twin principles to enable individualized monitoring in clinical contexts. The overarching aim remains the integration of *mIRror* within national healthcare pathways to deliver accessible and privacy-preserving diagnostic support.

Acknowledgments

This research was funded by the National Center for Scientific and Technical Research (CNRST) of Morocco under the 'PhD-Associate Scholarship –PASS' program.

References

[1] F. Bray, M. Laversanne, H. Sung, J. Ferlay, R. Siegel, I. Soerjomataram, A. Jemal "Global cancer statistics 2022: GLOBOCAN estimates of incidence and mortality worldwide for 36 cancers in 185 countries," *CA A Cancer J Clinicians*, vol. 74, no. 3, pp. 229–263, May 2024, doi: 10.3322/caac.21834.

[2] P. L. Bhukya and N. Thakur, Eds., *Nanoparticles in cancer theranostics: current progress in cancer management*, First edition. Boca Raton, FL: Taylor and Francis, 2025.

[3] D. J. Ahnen, S.W. Wade, W.F Jones, R. Sifri, S. Mendoza, J. Greenaymer, S. Guiffre, J. Axilbund, A. Spiegel "The Increasing Incidence of Young-Onset Colorectal Cancer: A Call to Action," *Mayo Clinic Proceedings*, vol. 89, no. 2, pp. 216–224, Feb. 2014, doi: 10.1016/j.mayocp.2013.09.006.

[4] T. J. Caverly, E. A. Kerr, and S. D. Saini, "Delivering Patient-Centered Cancer Screening," *American Journal of Preventive Medicine*, vol. 50, no. 1, pp. 118–121, Jan. 2016, doi: 10.1016/j.amepre.2015.08.003.

[5] R. A. Smith, S. W. Duffy, R. Gabe, L. Tabar, A. M. F. Yen, and T. H. H. Chen, "The randomized trials of breast cancer screening: what have we learned?," *Radiologic Clinics of North America*, vol. 42, no. 5, pp. 793–806, Sep. 2004, doi: 10.1016/j.rcl.2004.06.014.

[6] H. Hussein, E. Abbas, S. Keshavarzi, R. Fazelzad, K. Bukhanov, S. Kulkarni, F. Au., S. Ghai, A. Alabousi, V. Freitas "Supplemental Breast Cancer Screening in Women with Dense Breasts and Negative Mammography: A Systematic Review and Meta-Analysis," *Radiology*, vol. 306, no. 3, p. e221785, Mar. 2023, doi: 10.1148/radiol.221785.

[7] R. G. Blanks *et M. G. Wallis, R. Alison*, O. Kearins, J. Jenkins, J. Patnick, R. M. Given-Wilson "Impact of Digital Mammography on Cancer Detection and Recall Rates: 11.3 Million Screening Episodes in the English National Health

Service Breast Cancer Screening Program," *Radiology*, vol. 290, no. 3, pp. 629–637, Mar. 2019, doi: 10.1148/radiol.2018181426.
[8] B. K. Dunn, S. Woloshin, H. Xie, and B. S. Kramer, "Cancer overdiagnosis: A challenge in the era of screening," *Journal of the National Cancer Center*, vol. 2, no. 4, pp. 235–242, Dec. 2022, doi: 10.1016/j.jncc.2022.08.005.
[9] N. Kosus, A. Kosus, M. Duran, S. Simavli, and N. Turhan, "Comparison of standard mammography with digital mammography and digital infrared thermal imaging for breast cancer screening," *J Turkish German Gynecol Assoc*, vol. 11, no. 3, pp. 152–157, Sep. 2010, doi: 10.5152/jtgga.2010.24.
[10] D. Kesztyüs, S. Brucher, C. Wilson, and T. Kesztyüs, "Use of Infrared Thermography in Medical Diagnosis, Screening, and Disease Monitoring: A Scoping Review," *Medicina*, vol. 59, no. 12, p. 2139, Dec. 2023, doi: 10.3390/medicina59122139.
[11] *E. Martín-Del-Campo-Mena, P. A. Sánchez-Méndez, E. Ruvalcaba-Limon, F. M. Lazcano-Ramírez, A. Hernández-Santiago, J. A. Juárez-Aburto, K. Y. Larios-Cruz, L. E. Hernández-Gómez, J. A. Merino-González, Y. González-Mejía "*Development and validation of an infrared-artificial intelligence software for breast cancer detection," *Exploration of Targeted Anti-tumor Therapy*, pp. 294–306, Apr. 2023, doi: 10.37349/etat.2023.00135.
[12] R. Bansal, S. Collison, L. Krishnan, B. Aggarwal, M. Vidyasagar, S. T. Kakileti, G. Manjunath "A prospective evaluation of breast thermography enhanced by a novel machine learning technique for screening breast abnormalities in a general population of women presenting to a secondary care hospital," *Front. Artif. Intell.*, vol. 5, p. 1050803, Jan. 2023, doi: 10.3389/frai.2022.1050803.
[13] J. A. M. Barboza, L. I. S. Souza, M. S. Cerqueira, P. R. D. Andrade, H. H. D. Santos, and J. J. D. A. Ferreira, "Skin temperature of middle distance runners after a maximum effort test," *Acta Sci. Health Sci.*, vol. 42, p. e48114, Jul. 2020, doi: 10.4025/actascihealthsci.v42i1.48114.
[14] J. Verstockt, S. Verspeek, F. Thiessen, W. A. Tjalma, L. Brochez, and G. Steenackers, "Skin Cancer Detection Using Infrared Thermography: Measurement Setup, Procedure and Equipment," *Sensors*, vol. 22, no. 9, p. 3327, Apr. 2022, doi: 10.3390/s22093327.
[15] International Academy of Clinical Thermology, "Medical Infrared Imaging Standards and Protocols," International Academy of Clinical Thermology, Jul. 2015. [Online]. Available: https://iactthermography.org/standards/medical-infrared-imaging/
[16] S. Collison, "Artificial Intelligence based breast thermography using radiomic feature extraction versus conventional manual interpretation of breast thermograms in the prediction of breast cancer: a multi-reader study," Feb. 02, 2023. doi: 10.1101/2023.01.31.23285320.
[17] American Academy of Thermology, "Guidelines for Breast Thermography," American Academy of Thermology, Clinical Guideline, 2012. [Online]. Available: https://www.holisticbreasthealth.com/wp-content/uploads/2014/01/AAT_Breast_Guidelines_8_12-2.pdf
[18] M. Charlton, S. A. Stanley, Z. Whitman, V. Wenn, T. j. Coats, M. Sims, J. P. Thompson "The effect of constitutive pigmentation on the measured emissivity of human skin," *PLoS ONE*, vol. 15, no. 11, p. e0241843, Nov. 2020, doi: 10.1371/journal.pone.0241843.
[19] Incropera, Frank P.; DeWitt, David P.; Bergman, Theodore L.; Lavine, Adrienne S., *Fundamentals of Heat and Mass Transfer*, 7th ed. Hoboken, NJ: Wiley, 2011.
[20] K. Sommer, B. Plez, J. Cohen-Campagne, M. Moniez, J. Neveu, M. Betoule, S. Bongard, F. Feinstein, L. Le Guillou, C. Juramy, E. Sepulveda, T. Souverin "StarDICE II: Calibration of an Uncooled Infrared Thermal Camera for Atmospheric Gray Extinction Characterization," *Sensors*, vol. 24, no. 14, p. 4498, Jul. 2024, doi: 10.3390/s24144498.
[21] "Novel Performance Evaluation of Thermal Camera Based on VOx Bolometer Focal Plane Array via Analysis of Sigma NETD, Mean NETD, and Roughness Index," *Sensors and Materials*, p. 1283, 2018, doi: 10.18494/SAM.2018.1913.
[22] Jian Ma, Pengchao Shang, Chen Lu, Safa Meraghni, Khaled Benaggoune, Juan Zuluaga, Noureddine Zerhouni, Christine Devalland , Zeina Al Masry "A portable breast cancer detection system based on smartphone with infrared camera," *Vibroengineering {PROCEDIA}*, vol. 26, pp. 57--63}, 2019, doi: 10.21595/vp.2019.20978.

[23] A. Rancea, I. Anghel, and T. Cioara, "Edge Computing in Healthcare: Innovations, Opportunities, and Challenges," *Future Internet*, vol. 16, no. 9, p. 329, Sep. 2024, doi: 10.3390/fi16090329.
[24] Z. Li, H. Zhao, B. Li, and Y. Chi, "SoteriaFL: A Unified Framework for Private Federated Learning with Communication Compression," 2022, *arXiv*. doi: 10.48550/ARXIV.2206.09888.
[25] J. Corral-Acero, F. Margara, M. Marciniak, C. Rodero, F. Loncaric, Y. Feng, A. Gilbert, J. F. Fernandes, H. A. Bukhari, A. Wajdan, M. V. Martinez, M. S. Santos, M. Shamohammdi, H. Luo, P. Westphal, P. Leeson, P. DiAchille, V. Gurev, M. Mayr, L. Geris, P. Pathmanathan, T. Morrison, R. Cornelussen, F. Prinzen, T. Delhaas, A. Doltra, M. Sitges, E. J. Vigmond, E. Zacur, V. Grau, B. Rodriguez, E. W. Remme, S. Niederer, P. Mortier, K. McLeod, M. Potse, E. Pueyo, A. Bueno-Orovio, P. Lamata "The 'Digital Twin' to enable the vision of precision cardiology," *European Heart Journal*, vol. 41, no. 48, pp. 4556–4564, Dec. 2020, doi: 10.1093/eurheartj/ehaa159.
[26] L. F. Silva*, D.C.M. Saade, G.O. Sequeiros, A.C. Silva, R.S. Bravo, A. Conci* "A New Database for Breast Research with Infrared Image," *j med imaging hlth inform*, vol. 4, no. 1, pp. 92–100, Mar. 2014, doi: 10.1166/jmihi.2014.1226.
[27] M. Sandler, A. Howard, M. Zhu, A. Zhmoginov, and L.-C. Chen, "MobileNetV2: Inverted Residuals and Linear Bottlenecks," in *2018 IEEE/CVF Conference on Computer Vision and Pattern Recognition*, Salt Lake City, UT: IEEE, Jun. 2018, pp. 4510–4520. doi: 10.1109/CVPR.2018.00474.
[28] A. Howard, M. Sandler, Bo Chen, W. Wang, L. Chen, M. Tan, G. Chu, V. Vasudevan, Y. Zhu, R. Pang, H. Adam, Q. Le "Searching for MobileNetV3," in *2019 IEEE/CVF International Conference on Computer Vision (ICCV)*, Seoul, Korea (South): IEEE, Oct. 2019, pp. 1314–1324. doi: 10.1109/ICCV.2019.00140.
[29] M. Tan and Q. Le, "EfficientNet: Rethinking Model Scaling for Convolutional Neural Networks," in *Proceedings of the 36th International Conference on Machine Learning*, K. Chaudhuri and R. Salakhutdinov, Eds., in Proceedings of Machine Learning Research, vol. 97. PMLR, Jun. 2019, pp. 6105–6114. [Online]. Available: https://proceedings.mlr.press/v97/tan19a.html
[30] M. Tan and Q. Le, "EfficientNetV2: Smaller Models and Faster Training," in *Proceedings of the 38th International Conference on Machine Learning*, M. Meila and T. Zhang, Eds., in Proceedings of Machine Learning Research, vol. 139. PMLR, Jul. 2021, pp. 10096–10106. [Online]. Available: https://proceedings.mlr.press/v139/tan21a.html
[31] B. Zoph, V. Vasudevan, J. Shlens, and Q. V. Le, "Learning Transferable Architectures for Scalable Image Recognition," in *2018 IEEE/CVF Conference on Computer Vision and Pattern Recognition*, Salt Lake City, UT: IEEE, Jun. 2018, pp. 8697–8710. doi: 10.1109/CVPR.2018.00907.